

Stanford University

Seasonal Precipitation and Patterns of Turbidity Along the California Coast

Nicholas Mascarello
Earth Systems 141: Remote Sensing of the Oceans
Professor Kevin Arrigo
Final Paper
March 19, 2018

Introduction

Turbidity is a defining characteristic of aquatic environments, both marine and freshwater. Fundamentally, turbidity is a measure of the relative clarity of water and is an optical characteristic. More specifically, it is a function of the amount of light scattered by suspended material present in a water sample (Leopold & Langbein, 1960). The more light that is scattered, the higher the measured turbidity. Both biotic (e.g. phytoplankton, algae, other microscopic organisms) and abiotic factors (sediments/silts, inorganic and organic compounds) have the potential to affect the level of turbidity in a given body of water. Whether biotic or abiotic in nature, particles must be light enough to remain suspended in the water column and scatter light to contribute to turbidity.

Abiotic particles capable of making water turbid can have a range of natural sources including erosion of bedrock, gradual breakdown of larger rocks as they are moved by wind, water or tectonic activity, and resuspension of fine grain substrate material. Anthropogenic activities like mining, dredging, deforestation, agriculture, coastal modification and construction also act as sources of fine particles that can drive changes in turbidity once they make their way into water. In marine settings, research has identified three main processes that drive changes in turbidity: (1) Transformation of debris flows and slides, (2) Sediment transport by river or melt water runoff, and (3) Resuspension of coastal sediment located on shelves or upper-slopes by oceanographic events such as storms, tides and waves (Normark & Piper, 1991).

In the context of marine environments, turbidity is a characteristic fundamental to ecosystem biology, dynamics and function (Henley et al., 2000). Some marine environments are naturally turbid (i.e. coastal mangrove forests), whereas others depend on water that is regularly clear and free of sediment. Given its overall influence on the characteristics of marine

ecosystems, abnormally high turbidity has been found to have a number of important implications. Studies have thoroughly documented the negative effects of turbid waters and sedimentation on many marine ecosystems such as coral reefs, salt marshes and other coastal habitats (Bulleri & Chapman, 2010; Coulombier et al., 2012; Fabricius, 2005; Rogers, 1990). Taxa specific studies have also evidenced the detrimental effects that regular exposure to turbidity can have on fish and other organisms (Leahy et al., 2011; Sobral & Widdows, 2000; Wellington et al., 2010). As a consequence, high turbidity can also lead to economic consequences, impacting fisheries, overall biological wellbeing and proper ecosystem function (Chesney et al., 2000; Henley et al., 2000).

Turbidity is monitored in a number of ways. One of the simplest sampling methods used within a body of water is the deployment of a Secchi disk, which integrates the measurement of turbidity over depth. Turbidity can also be assessed in individual samples by utilizing a probe with a photodiode capable of capturing scattered light. While these techniques are sufficient for small scale and localized monitoring, other methods are required when working at the regional scale. The advent of advanced satellite remote sensing technology has effectively enabled researchers to study turbidity over areas of significant geographic scale, such as a bay or contiguous stretch of coastline. Remote sensing algorithms have been developed to return the diffuse attenuation coefficient for downwelling irradiance at 490 nm ($K_d 490, m^{-1}$) from data collected by satellite sensors. Such algorithms rely on the empirical relationship of in situ measurements of $K_d 490$ and blue-green band ratios of remote sensing reflectance (Austin & Petzold, 1981). As such, $K_d 490$ values derived from remote sensing data can serve a proxy for aquatic turbidity. Satellites capable of producing $K_d 490$ data include CZCS, OCTS, MODIS-Aqua and Terra, MERIS, SeaWiFS, VIIRS and others.

There is an extensive body of scientific literature that has assessed patterns of coastal turbidity utilizing remote sensing data, particularly patterns that occur over seasonal and interannual time scales. Many studies have monitored turbidity in a particular geographic region over a period of time. Chen et. al used MODIS 250-m data covering estuaries in the Tampa Bay region and found significant interannual variation in overall turbidity, as well as other patterns in particular estuaries that were linked to seasonal changes in wind and tidal patterns (2007). Salidas et. al also used high resolution MODIS imagery to investigate offshore sediment plumes induced by coastal river runoff in central Chile (2012). Their work found strong seasonality in the geographic extent of nearshore turbidity, with coastal water being most turbid during periods of intense winter rainfall and river discharge (Saldías et al., 2012). Brodie et. al considered large flooding events along the eastern Australia coastline during an intense period of winter rain using satellite and in situ data and found that significant sedimentary and fertilizer runoff contributed to elevated turbidity (2010). Another study conducted on the Great Barrier Reef utilizing only in situ data supported the findings of Brodie et, al, concluding that average turbidity across all surveyed reefs was 13% lower during weeks that experienced low rainfall compared to those that experienced high rainfall (Fabricius et al., 2013). Collectively, these studies demonstrate that remote sensing is capable of assessing patterns in turbidity and suggest a correlation between the extent and severity of coastal turbidity and rainfall intensity.

Given the findings of others, this study aims to assess patterns in turbidity along the California Coast during the wet season and determine if there is discernable difference in overall turbidity (i.e. magnitude of mean $K_d 490$) between years of above versus below average rainfall across the state. Existing work has established connections between rainfall intensity and coastal turbidity within certain regions of California. For example, two studies using MODIS and

SeaWiFS reported a strong correlation between amount of precipitation within a San Diego area watershed and size of offshore sediment plume (Lahet & Stramski, 2010; Nezlin & DiGiacomo, 2005). These studies also reported that El Niño events usually correspond to higher turbidity in the waters off the Southern California Coast. A similar study from across Southern California watersheds indicated that signatures of post-storm sediment plumes offshore were strongest within two days of heavy periods of rain because the precipitation was responsible for carrying fine sediments from land to sea (Nezlin & DiGiacomo, 2005) In the San Francisco Bay region, Ruhl et. al used a combination of in situ measurement and satellite data to suggest that high tidal events and large freshwater discharges during the rainy season are responsible for creating sediment plumes that span throughout the northern bay (2001).

This prior research has considered trends in turbidity only at regional scales along California's coast. An online literature review did not return any papers that evaluated turbidity in the waters of the entire state using remote sensing data. Therefore, this paper makes use of MODIS Aqua imagery to assess changes in turbidity during California's wet season from year to year. Specifically, distinct patterns in turbidity from years characterized by above and below average precipitation are presented. California has experienced periods of extended drought followed by rainy seasons with greater than normal precipitation throughout the last decade. Thus, the period from 2006-2017 offers a suitable window to evaluate how statewide rainfall influences coastal turbidity. Given that prior work has demonstrated the effect of heavy rainfall on sediment plumes and offshore turbidity, mean $K_d 490$ values from the coastal waters of California are expected to be higher in the years with above average precipitation and lower in years with below average precipitation.

Methods

Rainfall & El Niño Data

To determine the influence of statewide rainfall patterns on coastal turbidity, two datasets were utilized in this study. First, rainfall data were obtained from the National Weather Service's Advanced Hydrologic Prediction Service¹. Statewide maps showing departure from normal (in percentage) in yearly rainfall totals for each water year² from 2006-2017 were created using the AHPS website (Figure 1). The 2006-2017 time period was chosen due to data availability and because there were years with above average precipitation and below average precipitation included in this range. To facilitate analysis, years were grouped into two categories, wetter and drier, based on the visual appearance of the AHPS precipitation maps. The wetter years were 2006, 2010, 2011, 2016, 2017 and drier years were 2007, 2008, 2009, 2012, 2013, 2014, 2015. Given that related work has found that El Niño years generally correspond with higher Kd 490 in coastal waters, the mean Kd 490 values from the years characterized by moderate to very strong El Niño or La Niña conditions were grouped together to facilitate additional analysis. Information on El Niño/La Niña conditions was gathered from NOAA's Multivariate ENSO Index³ and the Golden Gate Weather Service's El Niño website⁴. Years with moderate to very strong El Niño conditions were 2009, 2010, 2015 and 2016 and years with moderate to strong La Niña's conditions were 2008, 2011, 2012.

¹ <https://water.weather.gov/precip/>

² Water year defined as time period between Oct. 1-September 30. As an example, the 2006 water year spanned Oct. 1 2005-Sept. 30 2006.

³ <https://www.esrl.noaa.gov/psd/enso/mei/>

⁴ <http://ggweather.com/enso/oni.htm>

Kd 490 Data

Remote sensing data were obtained from NASA's OceanColor Web.⁵ Using the Level 3 Data Browser, monthly images displaying diffuse attenuation coefficient at 490 nm (Kd 490) at 4km resolution were downloaded from MODIS Aqua imagery archive. California usually receives the vast majority of its precipitation from November through March (with heaviest rainfall concentrated in December-February), thus five images were downloaded for each year, one for each month from November to March. All images were visualized and analyzed in SeaDAS version 7.4. First, all five images for each year in the study were incorporated into a mosaic image that blended all of them together to show Kd 490 as it was measured throughout targeted time period. The geographic range of each mosaic was limited to the western coast of the United States to facilitate the desired analysis. Next, land masks were applied to each mosaic to ensure that the program would only collect Kd 490 data points from the ocean. Another mask was manually created with boundaries that incorporated the California coastline and nearshore waters from border to border (See Figure 2). All numerical data on mean Kd 490 were gathered from within the bounds of this mask and the same mask was applied to each mosaic image.

The statistics function within SeaDAS was used to collect values for minimum, maximum and mean Kd 490 values within the masked area of each wet season mosaic. These values were recorded and plotted in Microsoft Excel. To check for statistical significance among the Kd 490 averages for each year, a two-sample t-test was performed on the group of wetter year means and the group of drier year means. Another two-sample t-test was performed on the mean Kd 490 values for El Niño years versus those La Niña years.

⁵ <https://oceancolor.gsfc.nasa.gov/>

Results

A table summarizing the quantitative findings of this study can be found below (Table 1). In all processed images across all target years considered, mean Kd 490 values varied considerably from a low of 0.083 m^{-1} in 2015 to a peak of 0.1898 m^{-1} in 2014. Figure 3 displays the year to year variation in mean Kd 490. Figures 4-5 display all mosaics created in SeaDAS for this project grouped by drier and wetter years. Dry years tended to have lower mean Kd 490 values but notably, the highest yearly mean Kd 490 value was found for 2014, one of the driest years in this study. 2017, the wettest year, exhibited a mean Kd 490 slightly lower than that of 2014 (0.1776 m^{-1}).

Overall, mean Kd 490 was found to be higher within the masked coastal area for the wetter years compared to the drier years (Mean Kd 490_{dry} = 0.1175, Mean Kd 490_{wet} = 0.1370). In spite of this qualitative result, these means were not different enough to be statistically different. A two-sample t-test was performed on the two groups of mean Kd 490 values to compare wetter versus drier years. With a p value of 0.32, no significant difference was found. To check for significant differences between the mean Kd 490 values of El Niño versus La Niña years, another two-sample t-test was performed. No statistical significance was found between these groups means either ($p = 0.23$).

Discussion

Broadly speaking, the results of this study aligned with the expected outcomes. Although no statistical significance was reported, higher mean turbidity in coastal water was associated with greater precipitation across the state of California from November-March. No definitive

conclusions can be made based on this finding, but these results along with those of prior studies suggest that increased precipitation does play a role in increasing marine turbidity. The results of this study generally align with what others have found (e.g. Nezlin & DiGiacomo, 2005; Ruhl et al., 2001) but did not find any correlation between presence of El Niño or La Niña conditions and measured turbidity level.

The scope of this study did not enable the consideration of how other oceanographic and climate related factors could have influenced turbidity in tandem with precipitation. Given that mean $K_d 490$ values in drier years are not significantly different from mean $K_d 490$ values in wetter years, multiple factors are likely to contribute to coastal turbidity during the wet season. Abnormally high tidal patterns, changes in coastal productivity and strong storm activity are examples of oceanographic processes known to play role in turbidity. Future studies could improve on the methods of this work by incorporating additional datasets that could illustrate the effect of these and other processes.

Upwelling is another physical process known to influence coastal turbidity. California experiences seasonal upwelling and other research has explored connections between upwelling and water clarity using remote sensing data (Miller, 2009). While upwelling absolutely has the potential to influence turbidity in the coastal water column because of the primary productivity that it encourages, it is unlikely to play a major role during the months targeted in this study. Along the California Coast, upwelling generally peaks within or after the month of April, which was not one of the months captured in the mosaic images created for this research (García-Reyes & Largier, 2012).

This research uncovered a major anomaly in turbidity in 2014. The 2014 water year was one of the driest years in this study, yet its mosaic illustrated that coastal turbidity was higher

during this year than in any other, even compared to the 2017 water year, which saw California's wettest winter in well over a decade. 2014 turbidity appeared especially high along the central coast. A large plume of turbid water seen in the mosaic image extends throughout the San Francisco Bay region, reaching Kd 490 values upwards of 3.0 m^{-1} . After searching for scientific work and news articles discussing anomalous turbidity in the San Francisco Bay Region during the 2013-2014 winter, no conclusive evidence that could explain anomaly was found. Given the extent of the area effected by high turbidity, possible drivers could include especially high coastal productivity that clouded the water or significant sediment disruption and discharge due to human or tectonic activity.

This research illustrates that utilizing data from remote sensing can facilitate the assessment of seasonal patterns in turbidity and their connections to the relative amount of precipitation along the California Coast. While the results of this study offer some limited insight into the precipitation-turbidity connection, methodological improvements could enable more robust data collection and analysis in future studies. Imagery of higher resolution would incorporate more data points into the calculation of Kd 490 means and allow for consideration of turbidity patterns at an even smaller scale. Dividing the masked area within in which Kd 490 was assessed into smaller sections could also prove fruitful. Based on the results of this work and the findings of others, creating multiple masks with boundaries that are based on regional hydrological characteristics, watersheds, etc. is recommended. Doing so would allow for additional breakdown of the dataset and analysis of turbidity with respect to hydrological processes and rainfall patterns that are unique to discrete regions. Considering the important role that turbidity plays in the ecology and function of coastal ecosystems, further research into the

seasonal dynamics of turbidity is suggested. Given the ease of access of remote sensing imagery, it can undoubtedly play a role in future work of related scope.

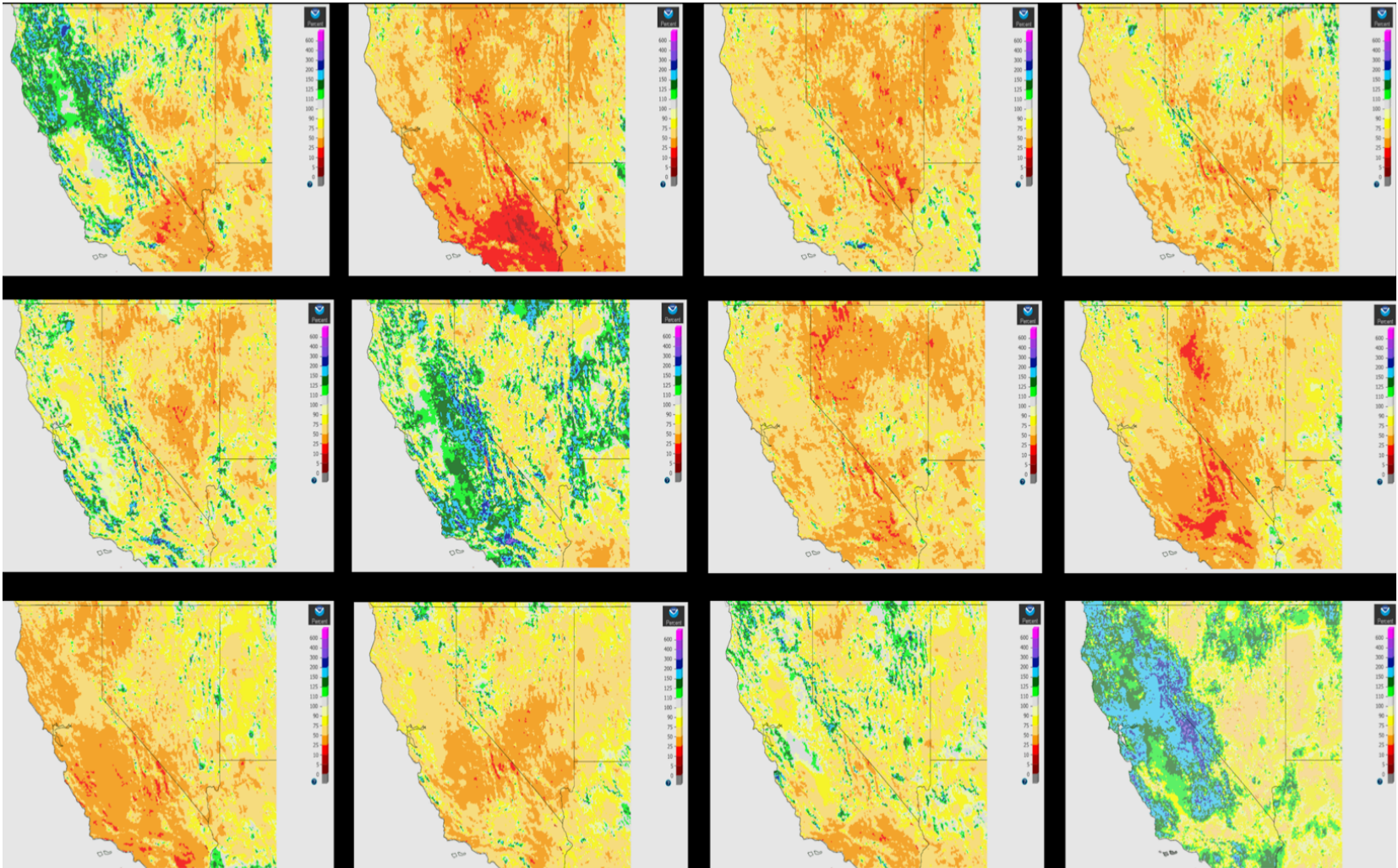


Figure 1: Departure from normal rainfall values (in percentage) for 2006 (upper left) – 2017 (lower right) water years. Wetter years: 2006, 2010, 2011, 2016, 2017; Drier years: 2007, 2008, 2009, 2012, 2013, 2014, 2015.

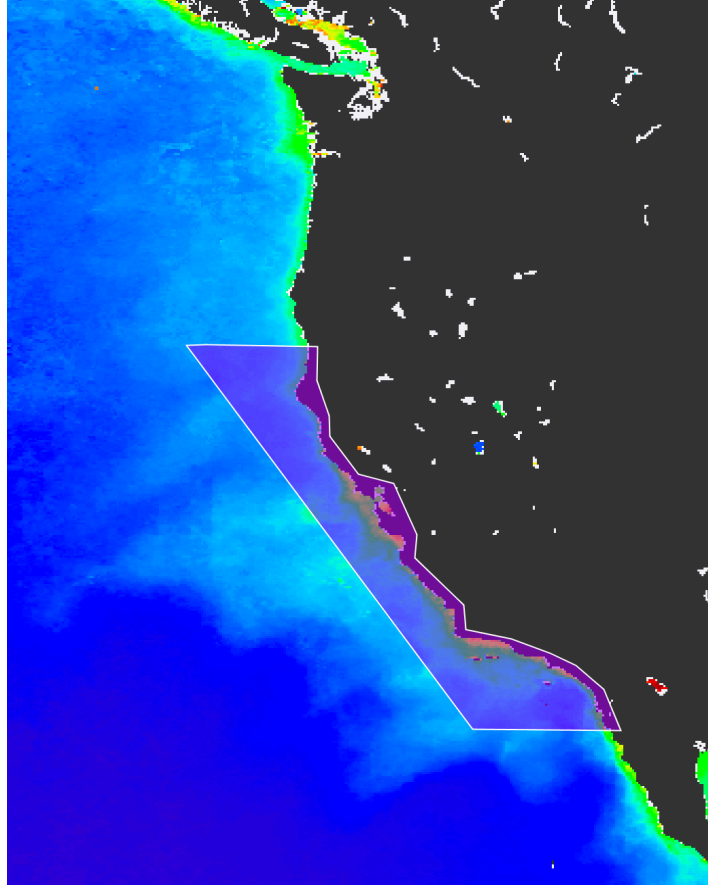


Figure 2: Example of mosaic image overlaid with a mask that marks the boundary of the region within which $K_d 490$ values were assessed using the SeaDAS statistics tool.

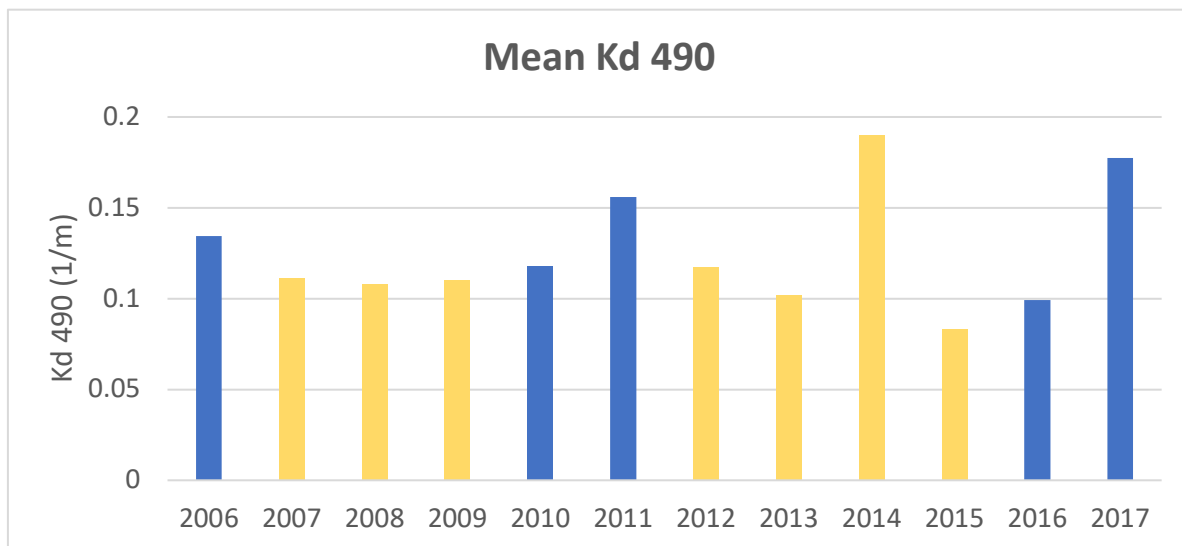


Figure 3: Mean $K_d 490$ across all years surveyed. Drier years are shown in yellow and wetter years are shown in blue.

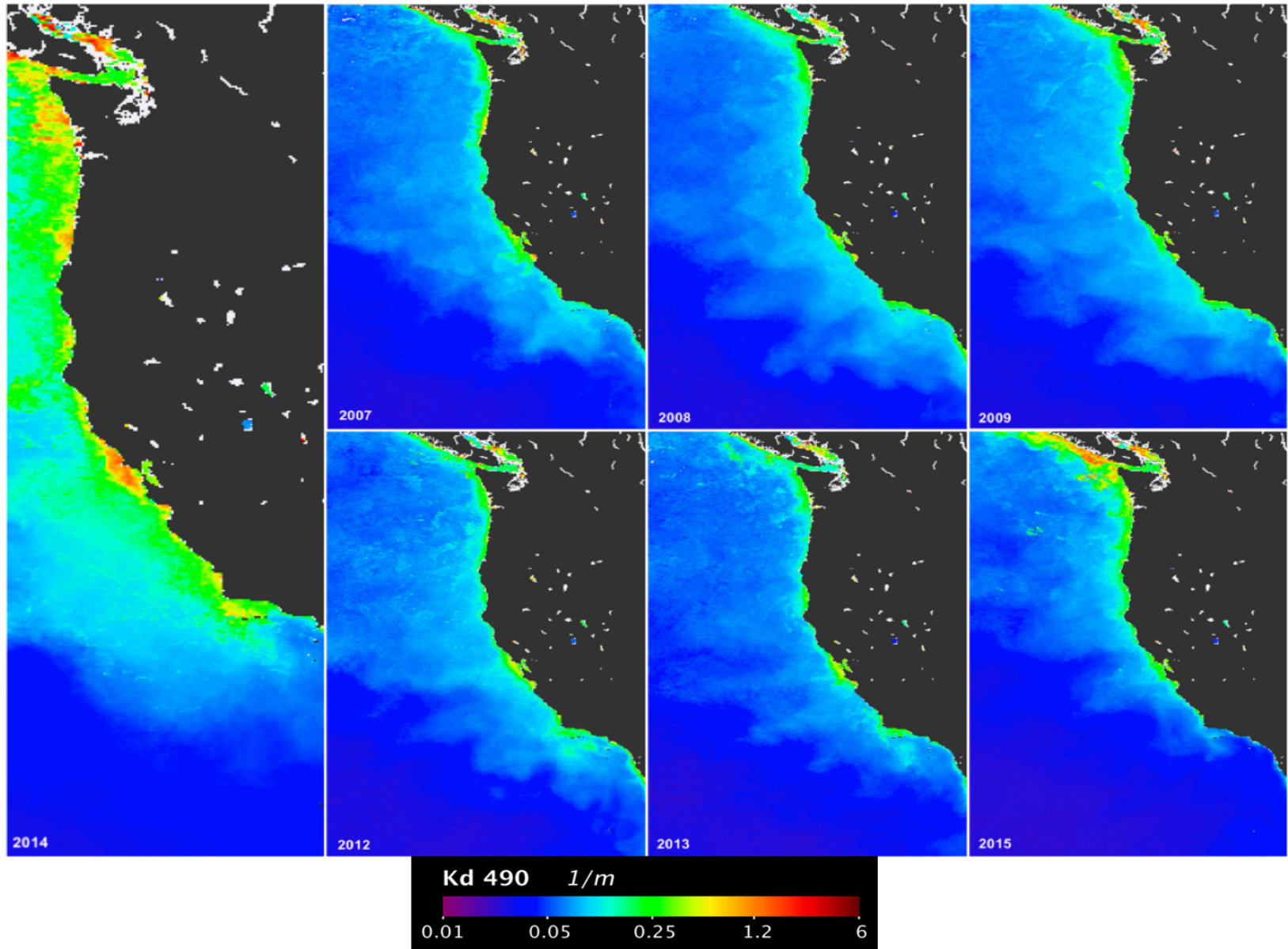


Figure 4: Mosaics representing $K_d 490$ values along the California Coast for the drier years. The 2014 mosaic is enlarged to illustrate that it is anomalous relative to the other dry years.

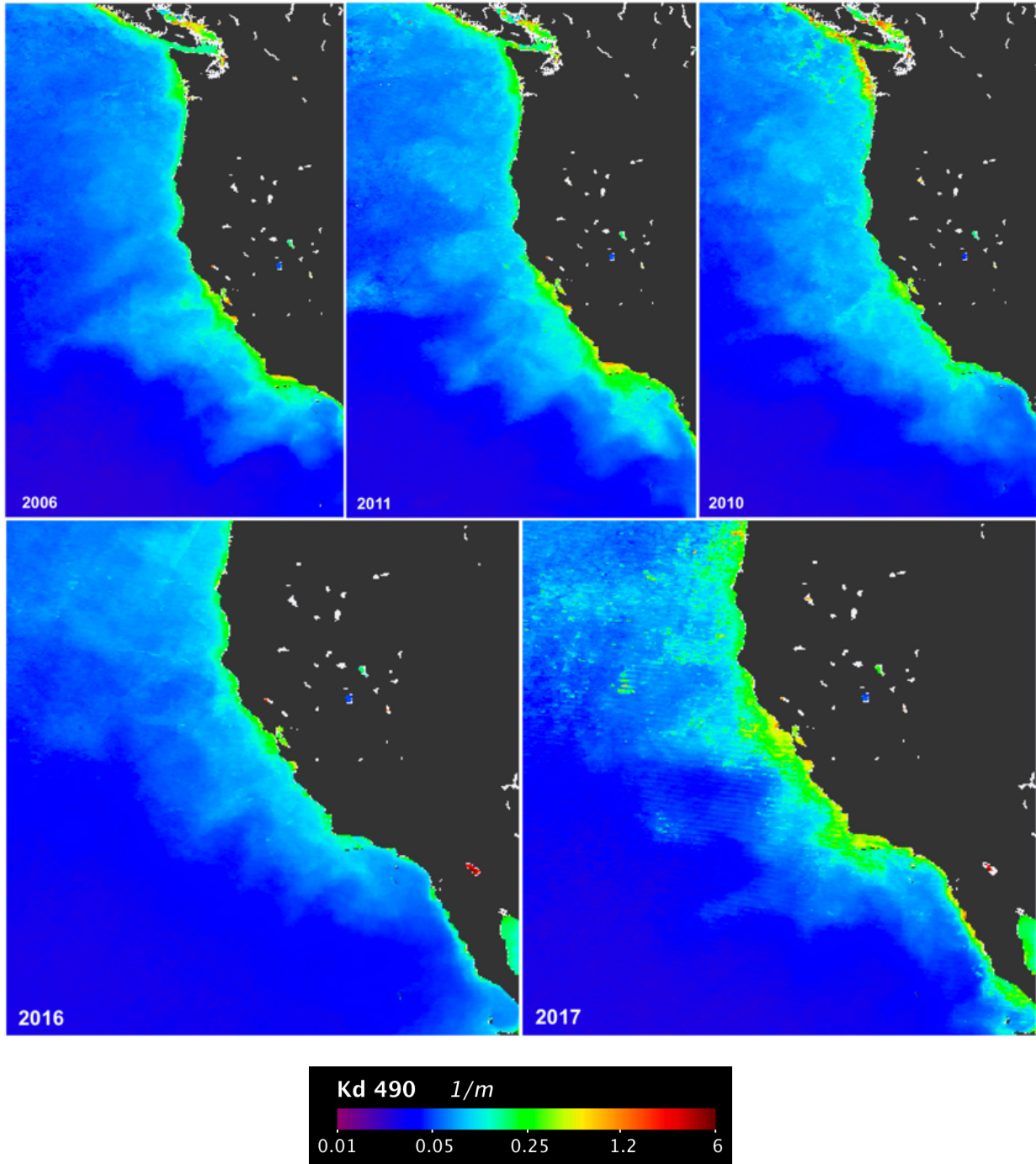


Figure 5: *Mosaics representing $K_d 490$ values along the California Coast for the wetter years.*

Year	Min Kd 490	Max Kd 490	Mean Kd 490
2006	0.0574	1.8496	0.1343
2007	0.0566	3.0088	0.1113
2008	0.0668	1.4706	0.1081
2009	0.056	1.2658	0.1104
2010	0.0495	1.1255	0.118
2011	0.0612	1.5692	0.1558
2012	0.0616	3.3162	0.1173
2013	0.0546	1.5877	0.1021
2014	0.0434	2.8288	0.1898
2015	0.0324	1.5227	0.0832
2016	0.0483	2.512	0.0994
2017	0.0496	3.282	0.1776
	Mean Min Kd 490	Mean Max Kd 490	Mean Kd 490
Drier Years	0.0531	2.1429	0.1175
Wetter Years	0.0532	2.06766	0.1370

Table 1: Numerical data collected in this study. All Kd 490 values reported in m^{-1} .

References

- Austin, R. W., & Petzold, T. J. (1981). The determination of the diffuse attenuation coefficient of sea water using the Coastal Zone Color Scanner. In *Oceanography from space* (pp. 239–256). Springer.
- Brodie, J., Schroeder, T., Rohde, K., Faithful, J., Masters, B., Dekker, A., ... Maughan, M. (2010). Dispersal of suspended sediments and nutrients in the Great Barrier Reef lagoon during river-discharge events: conclusions from satellite remote sensing and concurrent flood-plume sampling. *Marine and Freshwater Research*, *61*(6), 651–664. Retrieved from <https://doi.org/10.1071/MF08030>
- Bulleri, F., & Chapman, M. G. (2010). The introduction of coastal infrastructure as a driver of change in marine environments. *Journal of Applied Ecology*, *47*(1), 26–35.
- Chen, Z., Hu, C., & Muller-Karger, F. (2007). Monitoring turbidity in Tampa Bay using MODIS/Aqua 250-m imagery. *Remote Sensing of Environment*, *109*(2), 207–220. <https://doi.org/https://doi.org/10.1016/j.rse.2006.12.019>
- Chesney, E. J., Baltz, D. M., & Thomas, R. G. (2000). Louisiana estuarine and coastal fisheries and habitats: perspectives from a fish's eye view. *Ecological Applications*, *10*(2), 350–366.
- Coulombier, T., Neumeier, U., & Bernatchez, P. (2012). Sediment transport in a cold climate salt marsh (St. Lawrence Estuary, Canada), the importance of vegetation and waves. *Estuarine, Coastal and Shelf Science*, *101*, 64–75.
- Fabricius, K. E. (2005). Effects of terrestrial runoff on the ecology of corals and coral reefs: review and synthesis. *Marine Pollution Bulletin*, *50*(2), 125–146. <https://doi.org/http://dx.doi.org/10.1016/j.marpolbul.2004.11.028>
- Fabricius, K. E., De'ath, G., Humphrey, C., Zagorskis, I., & Schaffelke, B. (2013). Intra-annual variation in turbidity in response to terrestrial runoff on near-shore coral reefs of the Great Barrier Reef. *Estuarine, Coastal and Shelf Science*, *116*, 57–65.
- García- Reyes, M., & Largier, J. (2012). Seasonality of coastal upwelling off central and northern California: New insights, including temporal and spatial variability. *Journal of Geophysical Research: Oceans*, *117*(C3). <https://doi.org/10.1029/2011JC007629>
- Henley, W. F., Patterson, M. A., Neves, R. J., & Lemly, A. D. (2000). Effects of sedimentation and turbidity on lotic food webs: a concise review for natural resource managers. *Reviews in Fisheries Science*, *8*(2), 125–139.
- Lahet, F., & Stramski, D. (2010). MODIS imagery of turbid plumes in San Diego coastal waters during rainstorm events. *Remote Sensing of Environment*, *114*(2), 332–344. <https://doi.org/https://doi.org/10.1016/j.rse.2009.09.017>
- Leahy, S. M., McCormick, M. I., Mitchell, M. D., & Ferrari, M. C. O. (2011). To fear or to feed: the effects of turbidity on perception of risk by a marine fish. *Biology Letters*, *rsbl20110645*.
- Leopold, L. B., & Langbein, W. B. (1960). *A primer on water*. US Government Printing Office.
- Miller, P. (2009). Composite front maps for improved visibility of dynamic sea-surface features on cloudy SeaWiFS and AVHRR data. *Journal of Marine Systems*, *78*(3), 327–336.

- <https://doi.org/https://doi.org/10.1016/j.jmarsys.2008.11.019>
- Nezlin, N. P., & DiGiacomo, P. M. (2005). Satellite ocean color observations of stormwater runoff plumes along the San Pedro Shelf (southern California) during 1997–2003. *Continental Shelf Research*, 25(14), 1692–1711.
<https://doi.org/https://doi.org/10.1016/j.csr.2005.05.001>
- Normark, W. R., & Piper, D. J. W. (1991). Initiation processes and flow evolution of turbidity currents: implications for the depositional record.
- Rogers, C. S. (1990). Responses of coral reefs and reef organisms to sedimentation. *Marine Ecology Progress Series*, 62, 185–202. Retrieved from http://s3.amazonaws.com/academia.edu.documents/46819089/Responses_of_coral_reefs_and_reef_organism_20160626-14811-1stj2mo.pdf?AWSAccessKeyId=AKIAIWOWYYGZ2Y53UL3A&Expires=1489729331&Signature=xE2WnRUTVWjfZ94MnFLdqptOWE%253D&response-content-disposition=inline%25
- Ruhl, C. A., Schoellhamer, D. H., Stumpf, R. P., & Lindsay, C. L. (2001). Combined use of remote sensing and continuous monitoring to analyse the variability of suspended-sediment concentrations in San Francisco Bay, California. *Estuarine, Coastal and Shelf Science*, 53(6), 801–812.
- Saldías, G. S., Sobarzo, M., Largier, J., Moffat, C., & Letelier, R. (2012). Seasonal variability of turbid river plumes off central Chile based on high-resolution MODIS imagery. *Remote Sensing of Environment*, 123, 220–233.
<https://doi.org/https://doi.org/10.1016/j.rse.2012.03.010>
- Sobral, P., & Widdows, J. (2000). Effects of increasing current velocity, turbidity and particle-size selection on the feeding activity and scope for growth of *Ruditapes decussatus* from Ria Formosa, southern Portugal. *Journal of Experimental Marine Biology and Ecology*, 245(1), 111–125.
- Wellington, C. G., Mayer, C. M., Bossenbroek, J. M., & Stroh, N. A. (2010). Effects of turbidity and prey density on the foraging success of age 0 year yellow perch *Perca flavescens*. *Journal of Fish Biology*, 76(7), 1729–1741.